SUPPLEMENTARY INFORMATION

Implications of in-situ chalcogen substitutions in polysulfides for rechargeable batteries

Sanjay Nanda[a], Amruth Bhargav[a], Zhou Jiang[a], Xunhua Zhao[a], Yuanyue Liu[a], and Arumugam Manthiram*[a]

[a]*Materials Science and Engineering Program and Texas Materials Institute, The University of Texas at Austin, Austin, TX78712, USA*

*Corresponding author: Tel: +1-512-471-1791; fax: +1-512-471-7681.
E-mail address: manth@austin.utexas.edu (A. Manthiram)

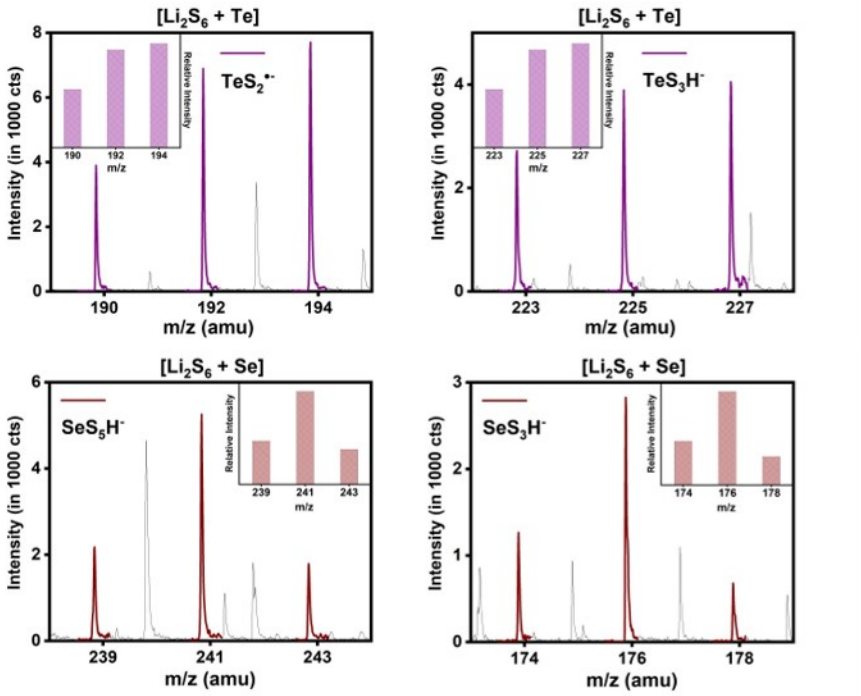

Figure S1. Mass spectra obtained with LC-MS for the [Li_2S_6 + Se] and [Li_2S_6 + Te] solutions, indicating the formation of a range of dianions and radical anions: SeS_5^{2-}, SeS_3^{2-}, TeS_3^{2-} and $TeS_2^{\bullet-}$, which are confirmed by the distinct isotopic signatures of Se and Te. The insets show the relative intensities of the peaks predicted by theory.

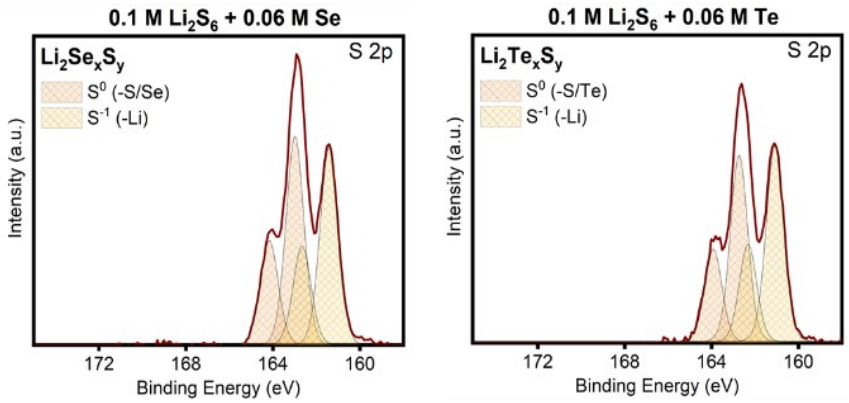

Name	Position	Raw Area	Area/(RSF*T*MFP)	%At. Conc
S 2p	162.91	3047.29	2694.23	93.63
Se 3d	55.31	278.107	183.196	6.37

Name	Position	Raw Area	Area/(RSF*T*MFP)	%At. Conc
S 2p	162.61	1783.11	1576.7	97.47
Te 3d	574.61	574.086	24.5304	1.52
Te 3d	585.11	384.267	16.3703	1.01

Figure S2. S 2p spectra for [Li_2S_6 + Se] and [Li_2S_6 + Te] show the bridging and terminal sulfur atoms in the polyselenosulfide and polytellurosulfide chains. Quantification of the S 2p spectra with corresponding Se 3d and Te 3d spectra reveal that the Se : S ratio is 0.07 and the Te : S ratio is 0.025 (a complete dissolution of Se and Te in the 0.1 M Li_2S_6 + 0.06 M Se/Te would imply a ratio of 0.1)

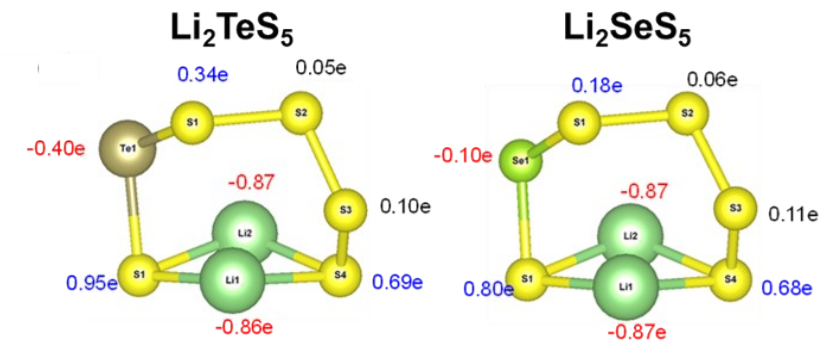

Figure S3. Bader charge analysis of Li_2TeS_5 and Li_2SeS_5 with negative and positive signs representing the charge loss and gain, respectively. The Te atoms are more positively charged than the Se atoms on account of the larger difference in Pauling electronegativity between Te and S (0.48) compared to that between Se and S (0.03).

Figure S4. Change in color of polypropylene separator from white to yellow due to polysulfides seeping in from the [Li_2S + 0.1 S] cathode and from white to brown due to polyselenosulfides seeping in from the [Li_2S + 0.1 Se] cathode. The separator shows no such color change with the [Li_2S + 0.1 Te] cathode.

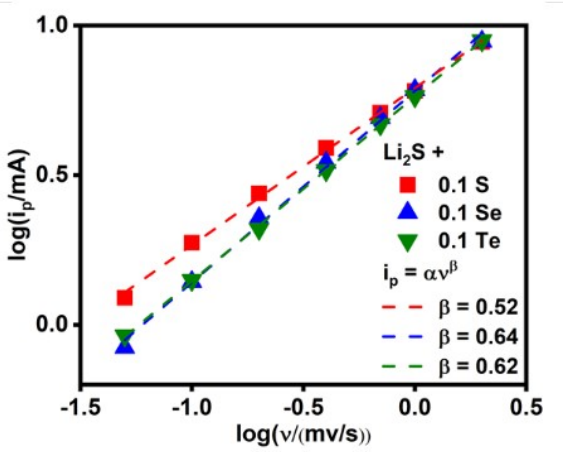

Figure S5. Log of peak currents in mA (i_p) plotted against log of scan rate in mv/s (ν) and fitted with a straight line to yield the kinetic descriptor β from the slope. The value of β increases from 0.52 to 0.64 with the introduction of Se, which indicates an improvement in redox kinetics.

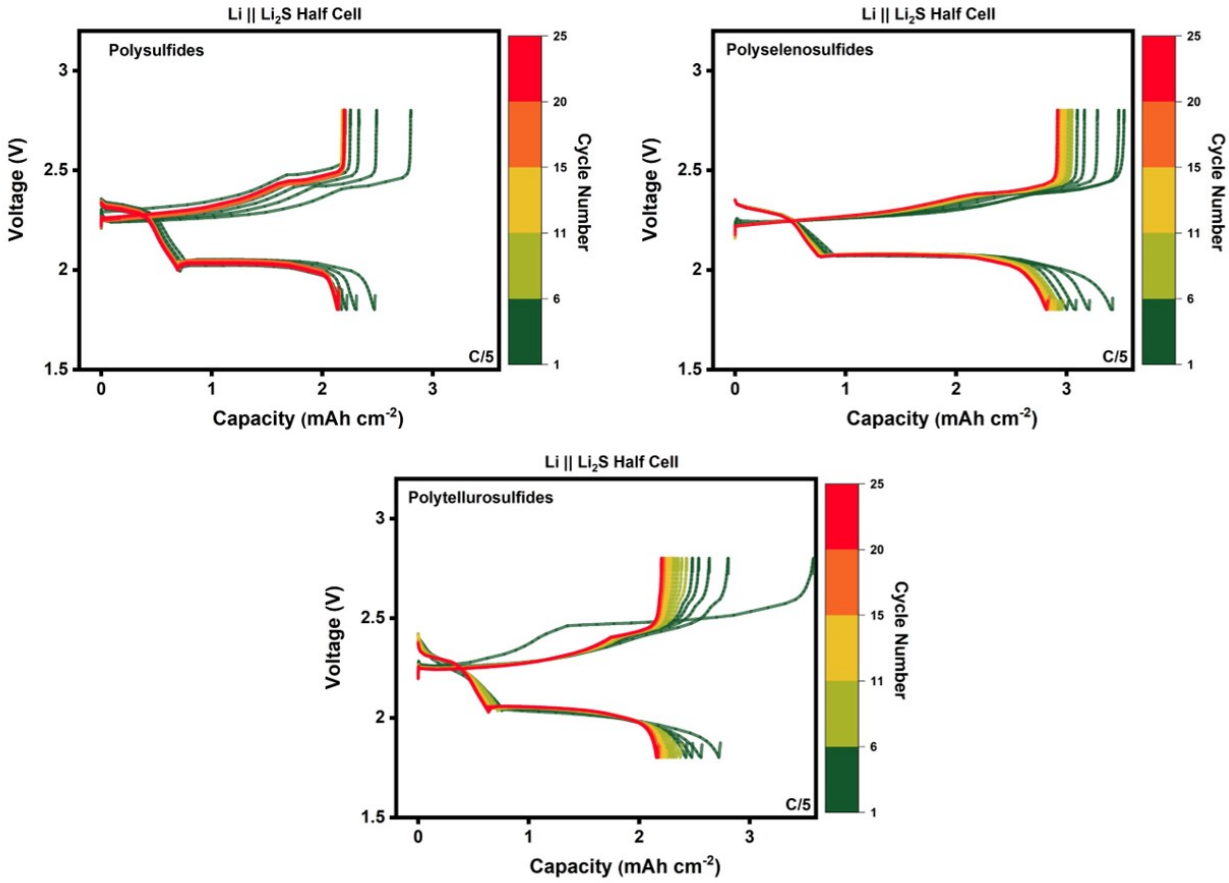

Figure S6. Charge-discharge plots for the first 25 cycles for Li || Li_2S half cells with 0.1 S (polysulfide), 0.1 Se (polyselenosulfide), and 0.1 Te (polytellurosulfide) additives, indicating the improvement in cathode utilization and overpotentials with the addition of selenium. The low Coulombic efficiency with 0.1 Te additive in the first cycle can be explained by the side reaction of elemental tellurium with polysulfides to form polytellurosulfides, which appears as an abnormally high charge capacity.

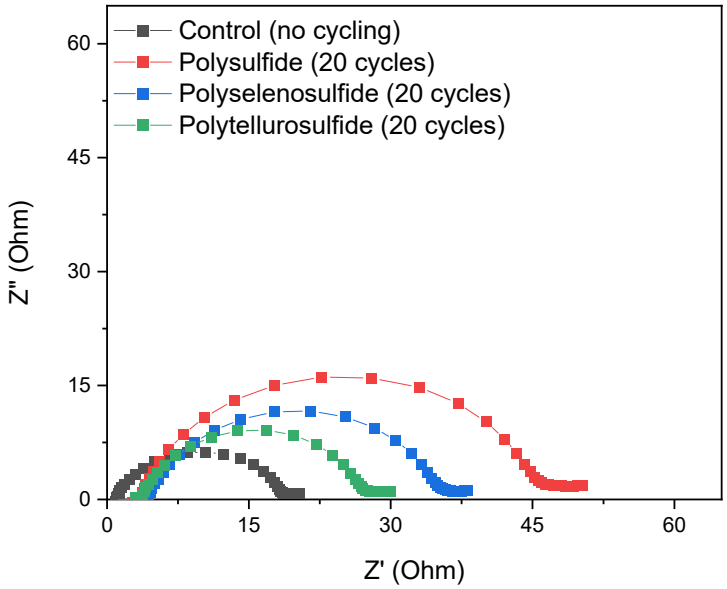

Figure S7. Electrochemical impedance spectroscopy of Li || Li symmetric cells with electrolytes containing polysulfide, polyselenosulfide, and polytellurosulfide additives after 20 cycles of lithium plating and stripping at 2 mA cm^{-2} and 2 mAh cm^{-2}. The charge-transfer resistance R_{ct} decreases in the order polysulfides > polyselenosulfides > polytellurosulfides.

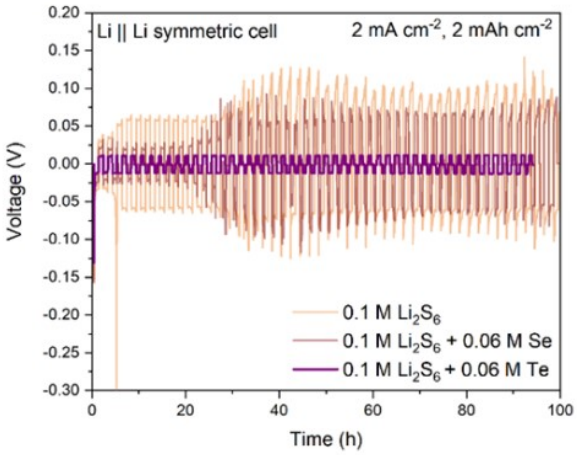

Figure S8. Overpotentials of lithium plating and stripping in Li || Li symmetric cells with electrolytes containing polysulfide, polyselenosulfide, and polytellurosulfide additives. The presence of polytellurosulfides enables the most stable overpotentials with cycling.

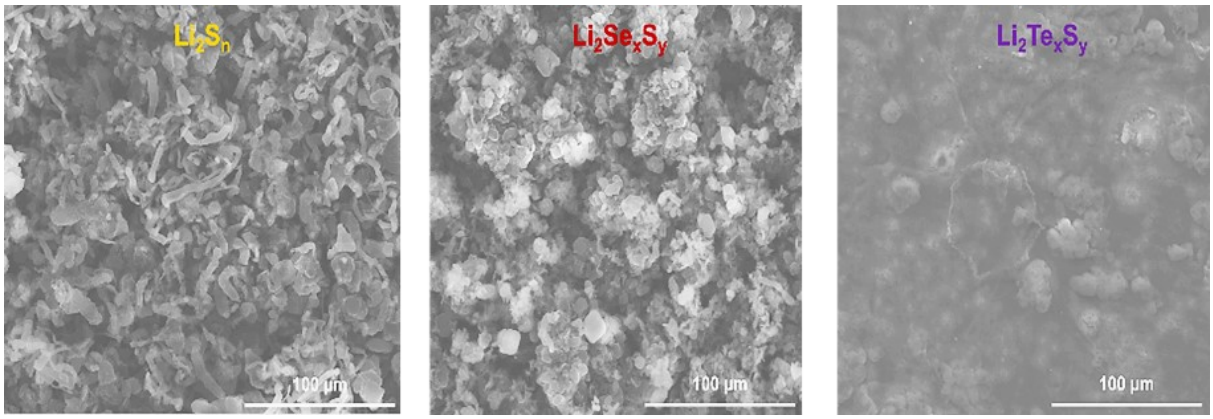

Figure S9. SEM images of deposited lithium in Li || Li symmetric cells with electrolytes containing polysulfide, polyselenosulfide, and polytellurosulfide additives. The presence of polytellurosulfides enables smooth, planar, and homogeneous deposition of lithium, in contrast to the high-surface area mossy growths observed with polysulfides and polyselenosulfides.

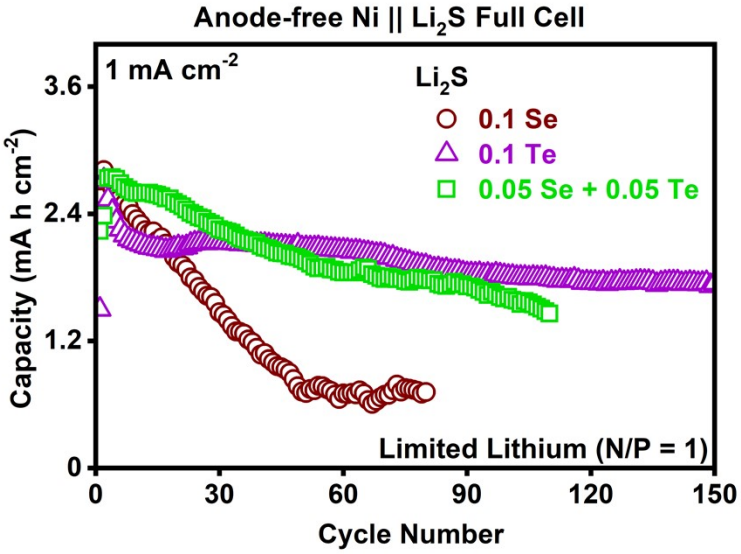

Figure S10. Capacity retention of an anode-free Ni || Li_2S full cell employing 0.05 Se + 0.05 Te additives, compared with just 0.1 Se and 0.1 Te additives. A synergetic effect is partially realized – initial discharge capacities are improved with 0.1 Te and cycling stability is improved with 0.1 Se. However, it is speculated that the instability of polyselenosulfides (SeS_2•- radical) precludes an improvement in cycle life that is comparable to that with 0.1 Te.

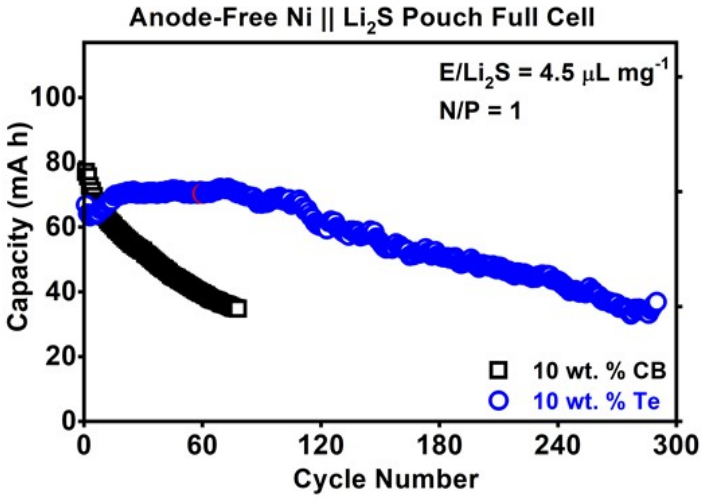

Figure S11. Electrochemical performances of anode-free Ni || Li_2S pouch full cells with 10 wt. % tellurium (Te : Li_2S molar ratio = 0.04) or 10 wt. % carbon black as cathode additives for nearly 300 cycles. The N/P ratio is equal to 1, the E/Li_2S ratio is 4.5 µl mg^{-1}, the Li_2S loading is 4.2 mg cm^{-2}, and the C-rate is C/10. The absence of a steep drop off in capacity indicates that the electrolyte does not dry out.

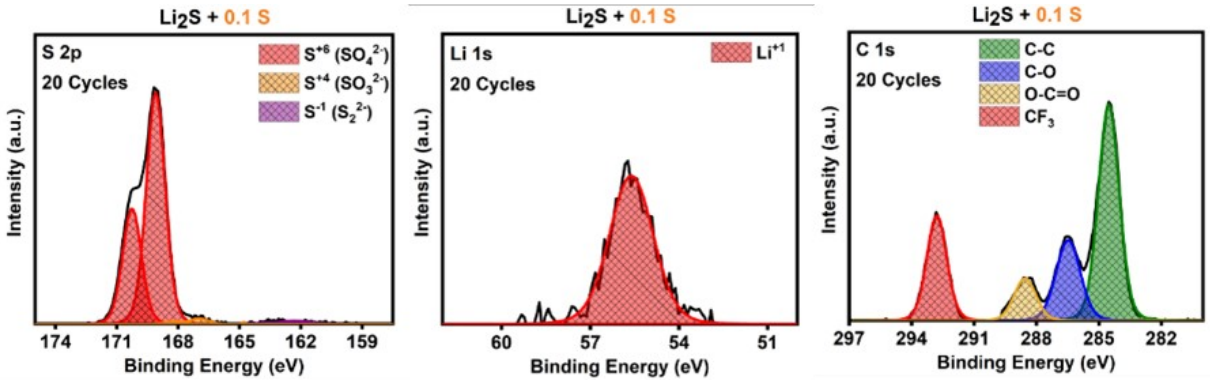

Figure S12. S 2p, Li 1s, and C 1s spectra for the lithium surface in anode-free Ni || [Li_2S + 0.1 S] full cell. The S 2p spectra is dominated by oxidized sulfur species from electrolyte decomposition, which is validated by the prominent peak for CF_3 groups in the C 1s spectra. The Li 1s spectra helps deconvolute the Se 3d spectra for the lithium surface in the cell with 0.1 Se additive.

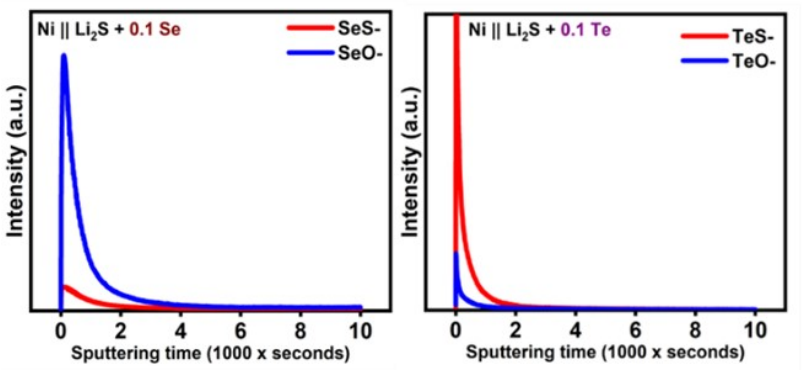

Figure S13. Comparing the depth profiles for SeS^-, SeO^-, TeS^-, and TeO^-, showing that selenium and tellurium atoms on the lithium surface are primarily bonded with oxygen and sulfur, respectively.

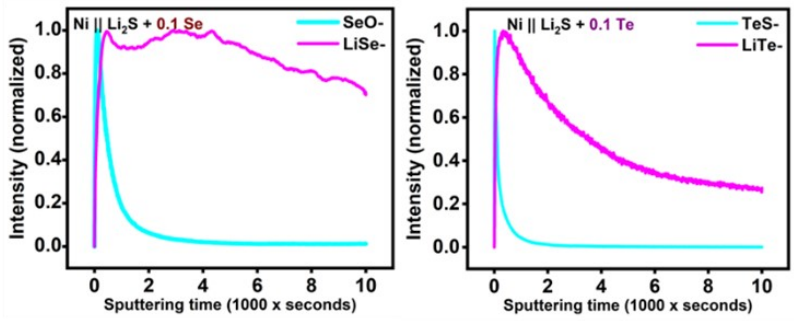

Figure S14. Normalized depth profiles for $LiSe^-$ and $LiTe^-$ reveal that fully reduced species such as Li_2Se and Li_2Te are present throughout the depth of the deposited lithium.

(a)

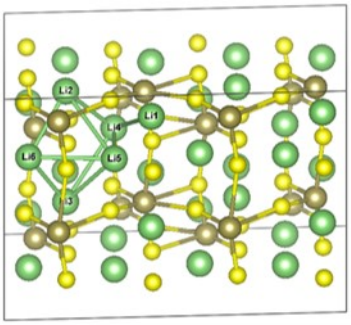

(b)

path	length (Å)	barrier (eV)
26	3.56	0.378
24	3.97	0.635
25	4.03	0.520
34	3.85	0.530
35	4.08	0.498
36	3.38	0.250
54	4.18	0.631
56	3.95	0.439

Figure S15. (a) Possible paths for Li^+-ion migration in Li_2TeS_3. One path (like 2-6) represents part of a complete pathway (like 2-6-3). (b) The chart shows barrier energies for all possible paths between adjacent Li atom sites based on single-ion migration.